ISSN 0010-5082, Combustion, Explosion, and Shock Waves, 2019, Vol. 55, No. 2, pp. 132–147. © Pleiades Publishing, Ltd., 2019.
Original Russian Text © I. Lytras, P. Koutmos, E. Dogkas.

# Reduced Kinetic Models for Methane Flame Simulations

**I. Lytras[a], P. Koutmos[a], and E. Dogkas[a]**

UDC 536.46+662.12

Published in *Fizika Goreniya i Vzryva*, Vol. 55, No. 2, pp. 11–28, March–April, 2019.
Original article submitted December 12, 2017; revision submitted April 24, 2018; accepted for publication May 23, 2018.

**Abstract:** The present paper describes the development of two reduced kinetic schemes suitable for multidimensional turbulent flame simulations in high-temperature oxidation of methane. Formal reduction of the USC Mech II C1-C4 detailed kinetic model by using the directed relations graph mechanism results in a 31-species derivative scheme for lean to near-stoichiometric conditions. To deduce a still shorter, simpler, and less stiff kinetic model, further species elimination is based on combined sensitivity and chemical time scale information to arrive at a 22-species scheme. The kinetic rates of lumped reactions are here expressed as simple Arrhenius rates, avoiding nonlinear algebraic combinations of excluded elementary steps or species. The accuracy is maintained by tuning pre-exponential constants in the global Arrhenius rate expressions and computing a range of target data. A more compact, quasi-global 14-species scheme is subsequently formulated by modeling fuel decomposition to a methyl radical pool, followed by $CH_3$ oxidation with O and OH toward $CH_2$ and CO, and retaining a full $CO/H_2/O_2$ subset. The C2-chain with recombination of $CH_3$ into $C_2H_6$ and production of $C_2H_2$ is also represented in both schemes. Equilibrium 0D and 1D propagating premixed flames and axisymmetric co-flowing lifted laminar jet flames are computed through an iterative validation process. Accompanying computations with the USC Mech II mechanism, as well as available experimental results, are exploited for optimization. The comparisons demonstrate that the derived schemes ensure satisfactory agreement with data over the investigated parameter space.

*Keywords*: reduced combustion chemistry, methane oxidation, laminar flames, chemical reaction schemes.

**DOI:** 10.1134/S0010508219020023

## INTRODUCTION

The achievement of fuel flexibility and emissions control represents an urgent target in the design and operation of current burner configurations. The need to achieve a profound understanding of the combustion processes involved and reduce optimization time has promoted the exploitation of Large Eddy Simulations (LES) as an adjunct to laboratory [1–3] and industrial-scale [4–6] experimental approaches.

An adequate representation of the combustion processes within these methodologies requires the consideration of a large number of fluid and chemical parameters and the description of chemical effects, such as pollutant emissions, autoignition, flame propagation speeds, and flash-back or blow-off events [1, 6]. This necessitates the use of sufficiently detailed chemistry and transport models [1, 5], an aspect that places a computational burden within turbulence-chemistry closures. Alternatively, reduced chemical schemes that are affordable within LES of complex configurations and provide a realistic description of thermochemical parameters are preferred [5–7].

[a]Laboratory of Applied Thermodynamics,
Department of Mechanical Engineering and Aeronautics,
University of Patras, Patras, 26504, Greece;
koutmos@mech.upatras.gr.

 

Various methodologies have been put forward to simplify a detailed mechanism. Starting with a comprehensive chemistry set [8], the first level of simplification through identification and elimination of elementary reactions and redundant species can be accomplished with the sensitivity analysis approach [9] or the method of directed relations graph (DRG) [1]. Subsequent reduction of this skeletal mechanism can be achieved through quasi-steady state assumptions for species and partial equilibrium for reactions by using, e.g., the quasi-steady-state approximation (QSSA) [10, 11], the computational singular perturbation (CSP) method [12], or the intrinsic low-dimensional manifold (ILDM) approach. These procedures can produce reduced chemistry sets with a varying degree of reduction in species and reactions, which is determined by the conflicting requirements for precision and economy.

Medium-size skeletal mechanisms involving 120–150 species and 17–25 reactions were developed specifically for methane by a number of researchers [13–16] and are widely used. Shorter reduced mechanisms of about 10–12 species and 10–15 reactions obtained by using the QSSA were proposed in [9, 17]. More rigorous reduction can result in even smaller-size methane mechanisms of 6–8 species and 5–7 global reactions [10, 11]. In such mechanisms, the rates of the resultant lumped reactions are explicitly expressed as elaborate algebraic combinations of the rates of the eliminated elementary reactions, whilst the concentrations of the excluded species required in these expressions are obtained from the original scheme through steady-state relations [9, 10].

Alternatively, semi-global kinetic schemes [4], which preserve a subset of the comprehensive mechanism, e.g., the $H_2$–$O_2$/CO/$CO_2$ system, employ one or more global fuel decomposition steps with tuned rate parameters and are attractive due to their straightforward implementation in simulation procedures. Still further simplifications can be achieved by global oxidation models, which include only a very limited number of species and reactions, with the kinetic rates adjusted to reproduce a number of pre-specified flame properties [17–19].

The present paper describes two reduced kinetic models of methane combustion: a 22-species scheme and a quasi- or semi-global 14-species model. The intention is to bridge the gap between extended reduced mechanisms involving a significant number of species and reactions [12, 14–16] and global schemes utilizing 6–8 species and 4–6 reactions [7, 8, 19]. One specific aim here is to avoid rate parameters of retained reactions being expressed in terms of complex nonlinear coupled algebraic combinations of the omitted elementary step rates and of the concentrations of the steady-state species, as commonly practiced in several works [10, 11, 17]. Such an approach usually results in an increased computational cost, more complicated implementation, and loss of accuracy in the (typically truncated) expressions of certain radicals that are essential for the description of flame properties. If reactions are omitted or lumped together, global Arrhenius rates are favored, with their pre-exponential constants optimized through calibration against target data, in a fashion similar to the semi-global scheme approach. A second additional issue addressed in the present model schemes is that the major and minor species and radicals retained in each mechanism specifically target to predict the temperature and pollutants, local extinctions and reignitions, and, quite significantly, offer the capability of calculating heat release and chemiluminescent species, through algebraic post-processing of simulation data [1].

Apart from its technical importance, methane is a popular laboratory model fuel from which quantitative information relevant to practical combustion can be extracted [5, 6, 17]. The present effort is also directly connected to on-going studies of lean stratified bluff-body stabilized flames [3]. The intention is to conveniently apply the reduced kinetic models within large eddy simulations of these flames.

0D and 1D freely propagating counter-flow premixed flames and axisymmetric co-flowing lifted laminar jet flames are computed. The encouraging validation tests lend support for possible extension of the approach to more complex hydrocarbons and alternative fuels of practical relevance.

## DESCRIPTION OF REDUCED MODEL MECHANISM DERIVATION

The chemical database employed was the USC Mech II C1–C4 detailed mechanism [8]. A skeletal 31-species 192-reactions model for methane–air lean mixtures, derived from the full kinetic model using the DRG methodology, was initially proposed by Egolfopoulos and Zhao [20]. This mechanism produced results in good agreement to the full USC II version and was used in various simulations including laminar Bunsen flames as reported in [21]. Subsequently, the effort was directed at producing a shorter 22-species and a quasi-global 14-species scheme. The 22-species and 14-species schemes are presented in the CHEMKIN format in the Appendix, whilst the participating species in each set are shown in the table.

**Table**

| Number of species | List of species |
|---|---|
| 31 | H, O, OH, $HO_2$ $H_2$, $H_2O$, $O_2$, CO, $CO_2$, HCO, $CH_2O$, C, CH, $CH_2$, $CH_2^*$, $CH_3$, $CH_4$, $CH_3O$, $CH_2OH$, $CH_3OH$, $C_2O$, $C_2H_2$, $H_2CC$, $C_2H_3$, $C_2H_4$, $C_2H_5$, $C_2H_5$, $C_2H_6$, HCCO, $CH_2CO$, $CH_2CHO$, $N_2$ |
| 22 | H, O, OH, $HO_2$, $H_2$, $H_2O$ $O_2$, CO, $CO_2$, HCO, $CH_2O$, $CH_2$, $CH_3$, $CH_4$, $CH_2OH$, $C_2O$, $C_2H_2$, $C_2H_3$, $C_2H_4$, $C_2H_5$, $C_2H_6$, $N_2$ |
| 14 | $H_2$, H, O, $O_2$, OH, $H_2O$, $CH_2$, $CH_3$, $CH_4$, CO, $CO_2$, $C_2H_6$, $C_2H_2$, $N_2$ |

In the 31-species scheme, all C3 and C4 species were excluded; most of methane reacts (at low pressures) with the radicals H, O, OH, and $HO_2$ to form a methyl radical pool. $CH_3$ is then rapidly consumed by the main radicals and $H_2$ through various possible paths, leading to the formation of $CH_3O$, $CH_3OH$, $CH_3O_2H$, $CH_2O$, CH, and $CH_2$. Subsequently, propagation reactions representing the main C1-chain reduce the size of partially oxidized molecules, e.g., from $CH_3O$ down through a straight path to $CH_2O$, HCO, CO, and $CO_2$. The recombination of methyl radicals into ethane $2CH_3(+M) \leftrightarrow C_2H_6(+M)$ was included and was followed by a complete C2 side chain toward $C_2H_5$, $C_2H_4$, $C_2H_3$, $C_2H_2$, $CH_2$, and CO. Furthermore, production and oxidation of CH, $CH_2$, and $CH_2^*$ species were also represented, and retention of relevant reactions involving these species resulted in a more accurate prediction of the flame speed, as well as CO and $CO_2$ concentrations, under fuel-rich conditions.

Additional reduction of the 31-species mechanism by applying a systematic DRG methodology produced significant errors in the reproduction of key flame parameters. Reduction could have also been undertaken by expressing quasi-steady-state species in terms of the remaining species by nonlinear coupled algebraic equations. Their iterative solution, however, would considerably burden the CPU time, whilst the truncation of species mass fractions, imposed to alleviate numerical implementation problems, would introduce further inaccuracies [5, 12, 13]. If simplification or combination of reactions is applied, global rates with simple kinetic parameters are adopted, excluding altogether intermediate elementary rates in the resulting global rate expressions. This offers clear advantages of stiffness reduction, higher processing speed, and possibility of implementation into large-scale computation codes. The rate coefficients of lumped reactions are fitted by comparing the performance of the mechanisms against a range of target data, an approach that has been previously followed by various investigators [4, 5, 7, 18].

Species removal from the 31-species mechanism was also guided by the results of a reduction study presented in [22]. A combined sensitivity and chemical time scale identification parameter (level of importance, LOI) was used there to permit the categorization and omission of species on the basis of their importance, sensitivity, and life time, assisted by the QSSA approach. As noted above, species retention in this work aimed also to facilitate comparisons between 3D turbulent simulations and experimental data obtained by optical imaging techniques. For instance, major or minor radicals or species, associated with QSSA-derived algebraic models, employed for calculating either chemiluminescence [$C_2H_2$ (related to the C2-chain) and $CH_2$], or heat release (CHO and $CH_2O$ [3]) are specifically retained, fully in the 22-species model and partly in the 14-species model. The combination of a suitably tailored reduced mechanism with an algebraic model for chemiluminescent species is likely to broaden the scope of direct comparisons between imaging measurements and computations. This capability makes these model schemes particular attractive for complex turbulent reactive simulations of experimental data.

The 22-species scheme (see Appendix) was derived by excluding the species $H_2O_2$, C, CH, $CH_3O$, $CH_3OH$, $H_2CC$, HCCO, $CH_2CO$, and $CH_2CHO$, as well as the associated reactions, from the 31-species scheme. Further, the pre-exponent in the rate of the methyl radical reaction with OH (reaction 51, $CH_3 + OH \leftrightarrow CH_2 + H_2O$) was increased by an order of magnitude to improve flame speed and ignition delay time predictions in richer mixtures. Species related to chemiluminescence modeling, such as $C_2H_2$ ($C_2H_6$) and $CH_2$, were retained. To represent fuel decomposition initiated by $O_2$ in the 22-species mechanism and emulate the autoignition behavior more appropriately, the reactions

$$CH_4 + O_2 \leftrightarrow CH_3 + HO_2,$$
$$CH_3 + HO_2 \leftrightarrow CH_3O + OH,$$

$$CH_3O + OH \leftrightarrow CH_2O + H_2O,$$
$$CH_2O + O_2 \leftrightarrow HCO + HO_2,$$
$$HCO + H_2O \leftrightarrow CO + H + H_2O,$$
$$CO + HO_2 \leftrightarrow CO_2 + OH$$

were grouped to formulate the global oxidation reaction [23]

$$CH_4 + H_2O_2 \rightarrow CO_2 + OH + H + H_2O.$$

Its reaction rate constants were tuned to reproduce autoignition times over the investigated range of conditions.

A more compact quasi-global 14-species model was subsequently formulated by applying further simplifications. The species $HO_2$, HCO, $CH_2O$, $CH_2OH$, $C_2O$, $C_2H_3$, $C_2H_4$, and $C_2H_5$ were now excluded on the basis of their LOI index [22] and sensitivity analysis. The consumption of methane by the main radicals (H, O, and OH) and the subsequent production of a methyl radical pool was retained. The C1-chain was continued by two methyl radical consumption reactions with O and OH. The former is represented by the global reaction

$$CH_3 + 2O \rightarrow CO + OH + H_2$$

(reaction 20 in the 14-species scheme, see Appendix), modeled through lumping reactions

$$CH_3 + O \leftrightarrow CH_2O + H,$$
$$CH_2O + O \leftrightarrow HCO + OH,$$
$$HCO + H \leftrightarrow CO + H_2$$

and adjusting its pre-exponent. $CH_3$ also reacts with OH to produce $CH_2$, which further reacts with O and $O_2$ to produce CO. In this quasi-global version, the most important kinetics $H_2$–$O_2$/CO–$CO_2$ was retained through 12 elementary reactions. In this shorter version, the C2-chain involving the recombination of the methyl radical into ethane was also represented to permit the evaluation of the $C_2H_2$ concentration. Ethane is oxidized to produce $C_2H_2$ via the modeled global reaction 23 in the 14-species scheme

$$C_2H_6 + 4H \rightarrow C_2H_2 + 4H_2$$

obtained by lumping reactions

$$C_2H_6 + H \leftrightarrow C_2H_5 + H_2,$$
$$C_2H_5 + H \leftrightarrow C_2H_4 + H_2,$$
$$C_2H_4 + H \leftrightarrow C_2H_3 + H_2,$$
$$C_2H_3 + H \leftrightarrow C_2H_2 + H_2$$

of the starting mechanism. Acetylene oxidation occurs mainly via the atomic oxygen attack through reaction 22:

$$C_2H_2 + O \leftrightarrow CO + CH_2.$$

Finally, the global reaction was employed to represent fuel decomposition initiated by reaction with $O_2$:

$$CH_4 + 2O_2 \rightarrow CO + 2OH + H_2O.$$

The introduced simplifications produced an unfavorable effect on the accuracy of the resulting schemes, and this was corrected through targeted tuning of the pre-exponential constants in selected reactions.

## VALIDATION OF REDUCED MECHANISMS. RESULTS AND DISCUSSION

The reduced kinetic models were optimized by computing several target flames and validated against prime performance indicators, such as adiabatic temperatures, flame speeds, species distributions, and autoignition times. Comparisons were performed against the USC mechanism, available experiments, and computations reported in the literature. 0D and 1D propagating premixed flames were computed over a range of conditions. More practical arrangements, such as counter-flow partially premixed jet flames spanning lean and ultra-lean mixtures and high strain rates, and also 2D axisymmetric co-flowing lifted laminar jet flames were assessed.

The iterative manual regression process adopted was made tractable by a relatively narrow parameter space covered in the tests for the two simplified schemes (equivalence ratio $\phi = 0.7$–$1.45$, pressure $p = 1$ atm, and reactant preheat temperature $T_0 = 300$–$650$ K). The tuning of the 22-species scheme involved adjustment of the pre-exponent of reaction 51 (see Appendix) and of the reaction rate constants in reaction 68, which represents methane decomposition by $O_2$. In the 14-species scheme, the pre-exponents in reactions 18, 19, 20, and 22, involving the production and destruction of $CH_2$, $CH_3$, $C_2H_2$, and $C_2H_6$, as well as the rate constants in reaction 28, representing fuel attack by $O_2$, were fitted to reproduce the autoignition times, laminar flame speeds, and species profiles over the above-given range of $\phi$ and the preheat temperature range $T_0 = 300$–$650$ K.

The 0D and 1D kinetic simulations of the target flames were completed by utilizing the software CHEMKIN II [24]. The computed axisymmetric co-flow jet flame setup was that previously used in [25, 26]. The central fuel jet was injected through a tube 4 mm in diameter with the wall thickness of 0.4 mm, which was placed at the axis of co-flowing air (50 mm in diameter). Both the central fuel mixture (65% of methane and 35% of nitrogen (65/35 flame) or 40% of methane and 60% of nitrogen (40/60 flame)) and the co-flowing air maintained an exit velocity of 35 cm/s. The software ANSYS 18 [27] was chosen for 2D computations, because the intention was to implement the developed kinetic models in associated 3D turbulent reactive flow simulations with this software. Detailed molecular transport prop-

erties, an optically thin radiation model, and a third-order MUSCL scheme were used, whilst stiff chemistry and a direct kinetic solver were employed for all computations. The computational domain (the burner is schematically shown in the inset in Fig. 8d) was meshed uniformly near the flame envelope with a total of about 250 000 cells, started upstream of the fuel inlet and extended to 25 nozzle diameters downstream to capture the lifted flame positions; in the radial direction, the computational domain covered eight nozzle diameters. Constant values of the variables were specified at inlet sections, taken from the experiments [25, 26]. A zero radial velocity and a zero gradient for axial velocity, temperature, and species concentrations were assumed on the axis and the open boundaries. A zero gradient was applied at the outflow.

Any significant discrepancies identified in these 2D runs led to modest readjustment of the leading fuel consumption rate parameters; these changes were, in turn, fed back to the 1D flame calibration runs. This iterative cycle produced the final set of the kinetic rate parameters given in Appendix.

Equilibrium calculations were first carried out with the USC, 22-species and 14-species schemes to verify the basic capability of reproducing flame temperatures and compositions under adiabatic 0D reactor conditions at an initial temperature and pressure of 298 K and 1 atm. Such results are not shown here for brevity. Some simplified schemes have been known to fail in this respect [5, 11], and the inclusion of significant radicals and intermediates together with the complete $H_2/O_2/CO/CO_2$ system adds to the quality of the 14-species set predictions.

The simplified mechanisms were next evaluated by computing autoignition delay times of methane–air mixtures at 1 atm, equivalence ratios $\phi = 0.7$–$1.3$, and initial autoignition temperatures $T_0 = 1000$–$2500$ K. The results calculated by the USC, 22-species and 14-species schemes and the 17-species reduced scheme of Lu and Law [12] for $\phi = 0.8$, 1.0, and 1.2, together with recent experiments by Hu et al. [28] are shown in Fig. 1. The successful reproduction of the ignition delay is directly related to the ability of any scheme to predict nonequilibrium transient combustion processes, such as ignition and extinction. This necessitates the good representation of primary combustion radicals, such as H, O, OH, $HO_2$, and $H_2O_2$ [1, 4, 7], an aspect that has been fully addressed in the 22-species mechanism and in part in the 14-species scheme. These comparisons indicate that the present models follow quite satisfactorily the trend and level of the target data and that both compare quite favorably with the 17-species reduced scheme of Lu and Law [12].

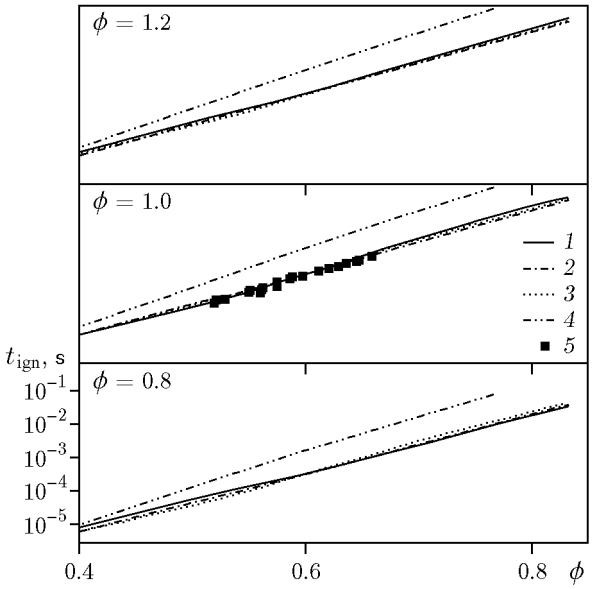


**Fig. 1.** Autoignition delay times predicted by different kinetic models ($\phi = 0.8$, 1.0, and 1.2): USC (*1*), 22-species model (*2*), 14-species model (*3*), 17-species model [12] (*4*), and experiment [28] for $\phi = 1.0$ (*5*).

The two schemes were subsequently tested by calculating unstretched laminar flame speeds, as well as species and temperature profiles in preheated freely propagating laminar 1D flames and comparing the results against the experimental data [28–30], the USC mechanism, and the 17-species reduced scheme of Lu and Law [12]. As the flame speed accounts for the diffusivity, exothermicity, and reactivity of the mixture, its accurate reproduction over a range of equivalence ratios represents a most stringent validation.

Figure 2 shows the flame propagation speed $v$ as a function of the preheat temperature. The predicted lean and stoichiometric parts of the curve (with a peak value of 0.382 m/s at $T_0 = 300$ K) agree reasonably well with the experimental values (0.365–0.387 m/s). Both proposed reduced schemes predict successfully the flame speed in the entire considered range of $\phi$ with deviations slightly increasing in the case of preheated reactants in the edge regions of the graph. The exhibited agreement with the USC mechanism and the results of Lu and Law [12] is quite encouraging even for the shorter 14-species model. An attempted 11-species scheme overestimated the data in the fuel-rich branch by more than 70%, and such a discrepancy could only be rectified through a parameterized correction of the pre-exponents of the leading reactions [5, 7, 18].

The profiles of the temperature $T$ and two selected species $X$, CO and OH, are compared in Fig. 3. The species profiles are close to the experimental data. Some

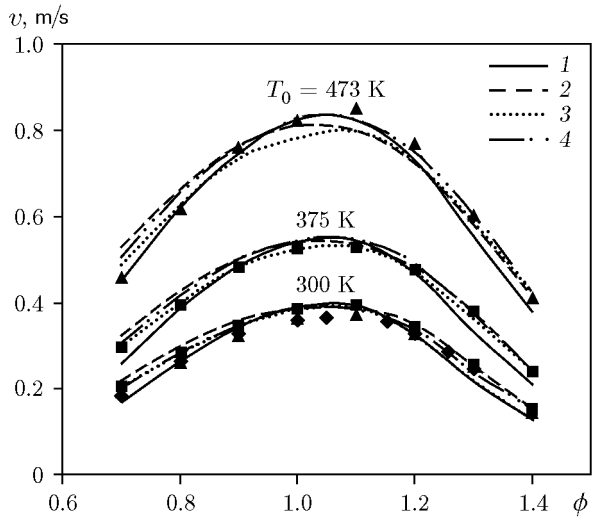


**Fig. 2.** Laminar flame speed for freely propagating premixed flames versus the equivalence ratio for $p = 1$ atm and different reactant preheat temperatures. Comparisons between the two reduced kinetic model calculations: 14-species model (*1*), 31-species model (*2*), 22-species model (*3*), and 17-species model [12] (*4*); the points show the experimental data of [28] (▲), [29] (◇), and [30] (■).

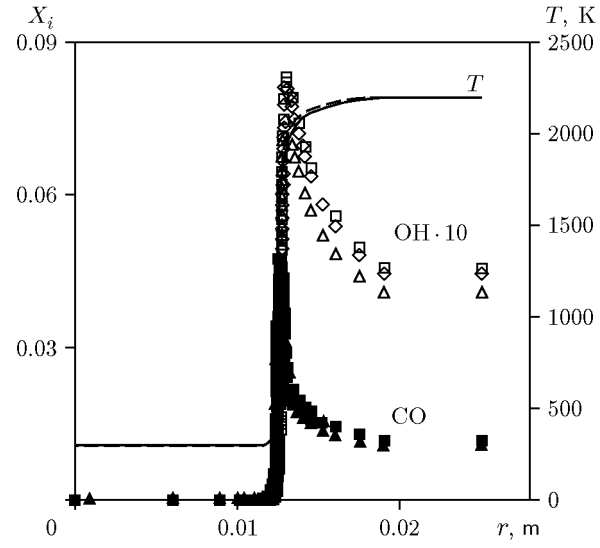


**Fig. 3.** Temperature and species (CO and OH) distributions across the reaction front of a 1D freely propagating flame ($\phi = 1$): USC (■ and □), 22-species model (◆ and ◇), and 14-species model (▲ and △).

moderate underprediction of the CO (and $CO_2$) concentration is observed for the quasi-global scheme. It has also been recognized by a number of researchers [4, 9] that such a satisfactory agreement cannot normally be achieved with only 2- or 6-step mechanisms and less than 8–9 species.

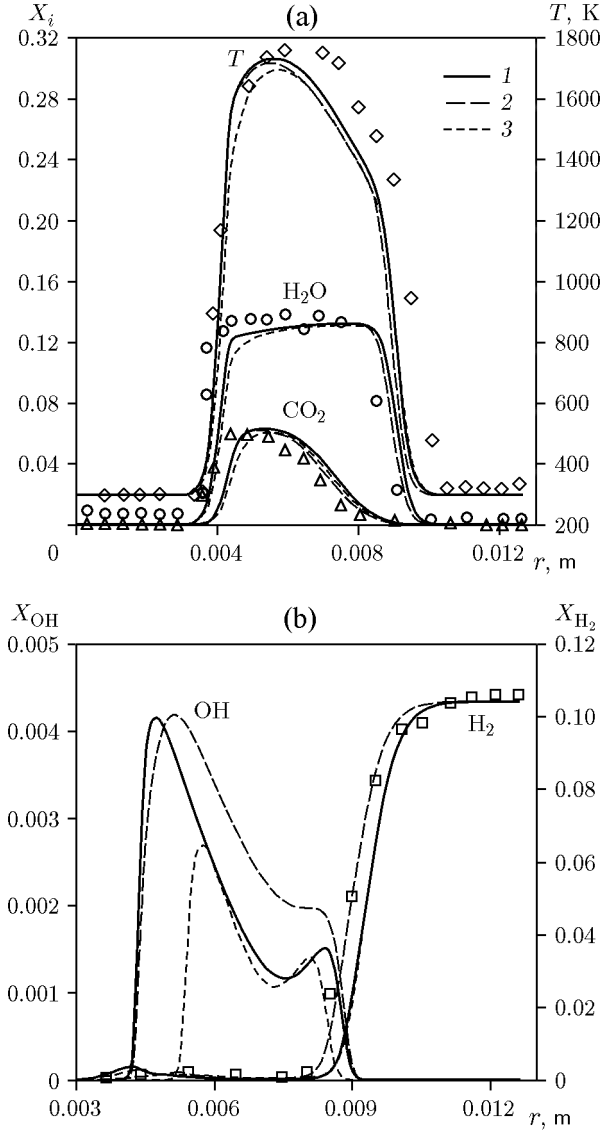


**Fig. 4.** Comparison of experimental and predicted temperature and species profiles for a lean opposed-jet flame [31]: $CH_4$–air ($\phi = 0.68$) and $H_2$–air ($\phi = 0.28$), strain 140 $s^{-1}$; USC (*1*), 22-species model (*2*), and 14-species model (*3*); (a) experimental data [31] for $T$, $H_2O$, and $CO_2$ (◇, ○, and △), respectively; (b) data for $C_2H_2$, OH, and $H_2$; experimental data for $H_2$ [31] (□).

1D stretched partially premixed flames produced by counter-flowing a lean ($\phi = 0.28$) $H_2$–air jet onto a $CH_4$–air jet with ultra-lean ($\phi = 0.43$ and 0.54) or lean to near-stoichiometric ($\phi = 0.68$ and 0.81) composition settings were experimentally and computationally investigated by Cheng et al. [31]. Such complex flames are of relevance to practical processes occurring under stratified operation of either direct injection spark ignition engines [14] or stratified and vitiated bluff-body flames [2, 3].

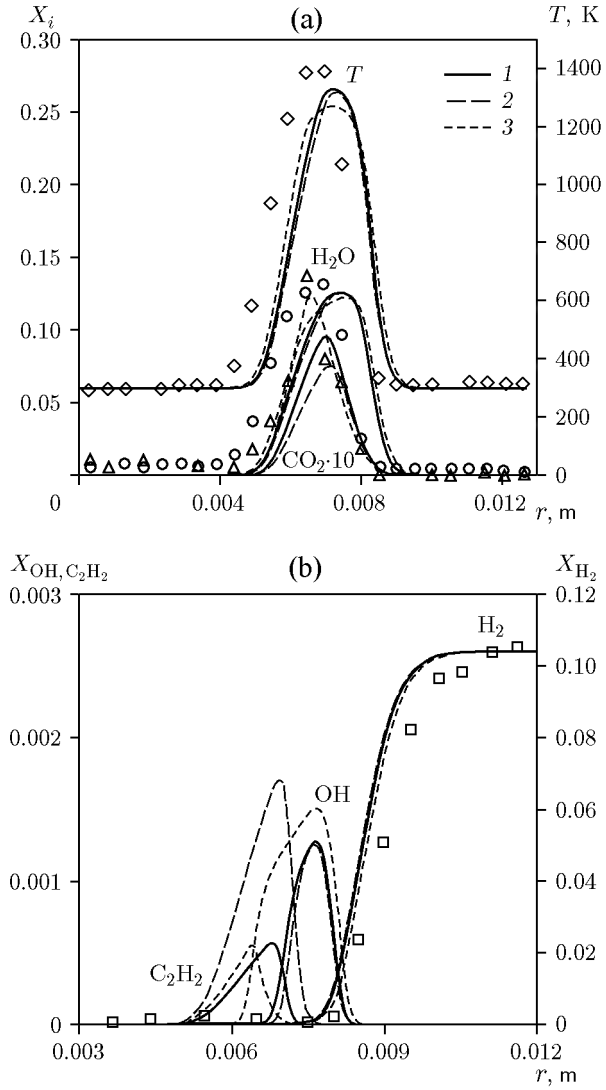


**Fig. 5.** Comparisons of experimental and predicted temperature and species profiles for a near-limit opposed-jet flame: $CH_4$–air ($\phi = 0.54$) and $H_2$–air ($\phi = 0.28$); strain 140 $s^{-1}$; USC (*1*), 22-species model (*2*), and 14-species model (*3*); (a) experimental data [31] for $T$, $H_2O$, and $CO_2$ (◇, ○, and △, respectively); (b) data for $C_2H_2$ and OH.

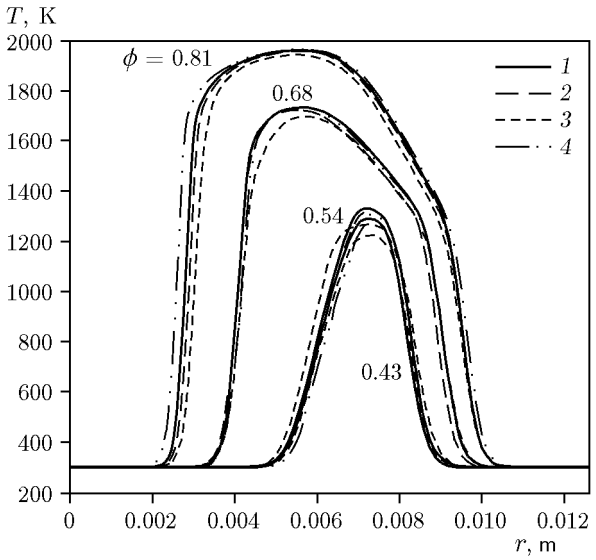


**Fig. 6.** Comparisons of the predicted temperature profiles for a range of diminishing values of $\phi$ for an opposed-jet flame: $CH_4$–air and $H_2$–air ($\phi = 0.28$); strain 140 $s^{-1}$; USC (*1*), 22-species model (*2*), 14-species model (*3*), and 17-species model [12] (*4*).

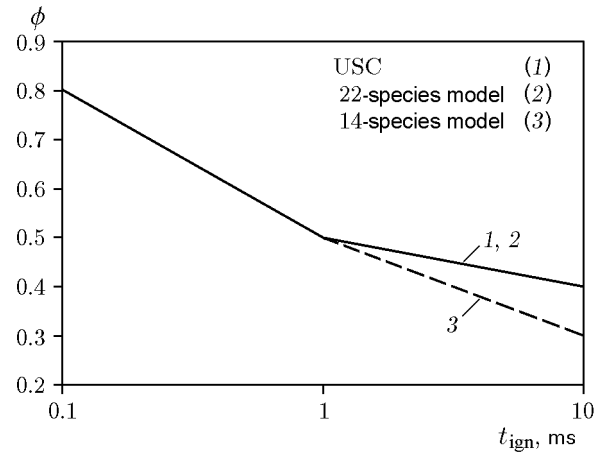


**Fig. 7.** Lean blow-out stability curve for $CH_4$–air mixtures at $p = 1$ atm and $T_0 = 300$ K.

The computations with the present schemes and the USC mechanism are compared with these experimental results in Figs. 4 and 5 for methane mixtures with $\phi = 0.68$ and 0.54 at a strain rate of 140 $s^{-1}$. Very good agreement with the measured temperature, $CO_2$, and $H_2O$ profiles is observed in Fig. 4a, denoting that the two model schemes accurately describe the flame penetration into the methane–air mixture. This is the result of the accurate prediction of the propagation speed over this specific range of $\phi$ (see Fig. 2).

It is encouraging that all experimental trends such as, e.g., the $H_2O$ plateau and the hydrogen side profiles, have been captured quite well. The 14-species mechanism ensures very satisfactory agreement in both temperature and species profiles as well. Overall comparisons suggest that minor species, important radicals such as H and OH, and intermediate hydrocarbons (see Fig. 4b) have also been captured well by the two reduced schemes.

The computations for the limiting flame condition of $\phi = 0.54$ are displayed in Fig. 5. Encouragingly, both the 22-species and the 14-species schemes have repro-

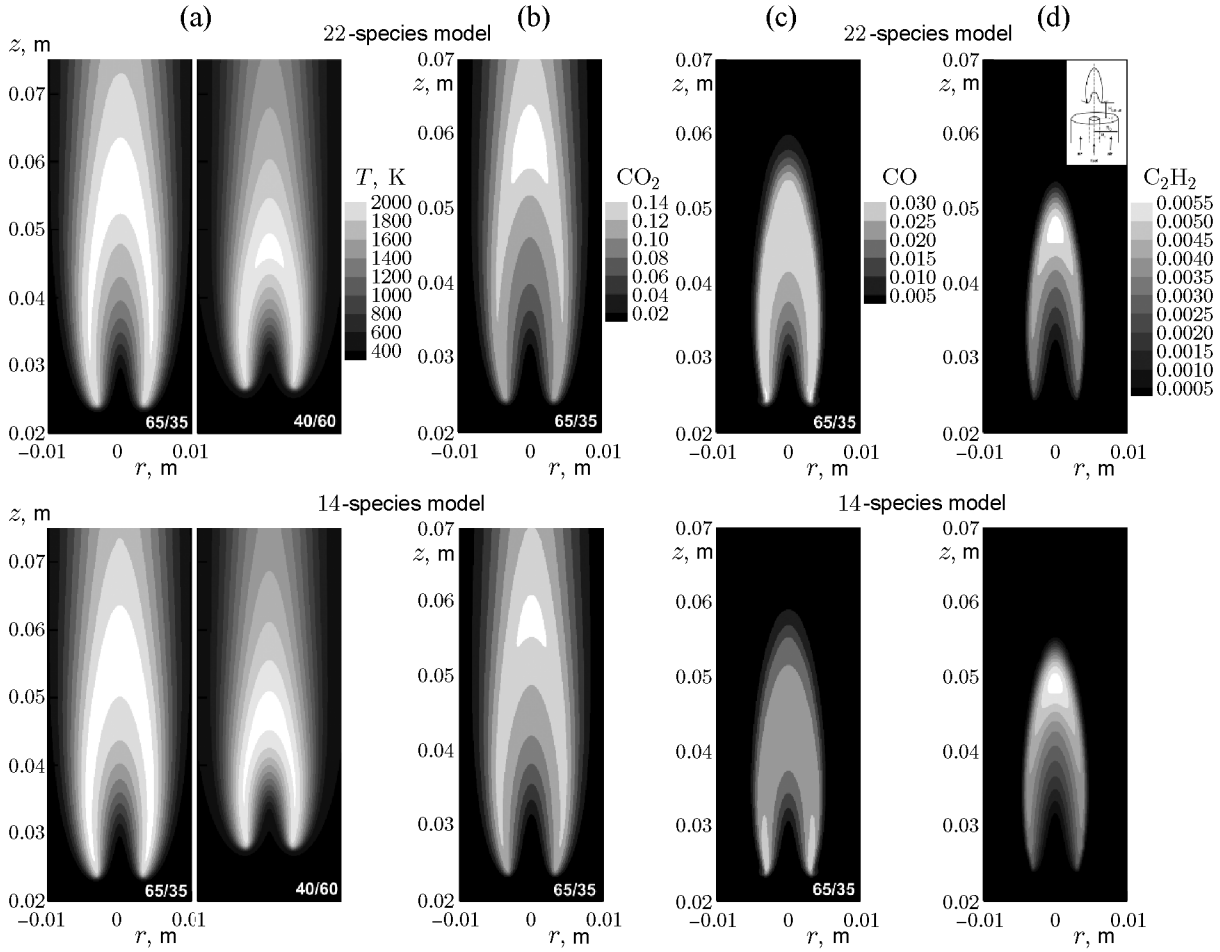


**Fig. 8.** Computations of temperature isotherm topologies for co-flowing jet flames [25, 26]: (a) temperature fields for 65/35 and 40/60 methane–nitrogen mixtures; (b)–(d) $CO_2$, CO, and $C_2H_2$ concentrations in a 65/35 flame; the computations are performed with the 22-species and 14-species models (the jet flame burner is schematically shown in the inset of Fig. 8d).

duced, both qualitatively and quantitatively, the drastic variations that resulted from reverting to a mixture that is very close to the lean flammability limit (sustaining reaction only by hydrogen stream dilution). The successful reproduction of these complex limiting flame patterns reflects the ability of the schemes to study behaviors related to ignition, extinction, and flash-back in practical laboratory flame burners [4, 5, 14]. Furthermore, the radicals and $C_2H_2$ included in both mechanisms are beneficial if correlations between 3D simulations and nonintrusive flame zone optical measurements, such as chemiluminescence or LIF images, are to be fruitfully exploited [5].

The predictions of the variations in the temperature profiles obtained as the equivalence ratio is reduced toward the limiting condition $\phi = 0.43$ are compared in Fig. 6 for the USC mechanism, the present two developed models, and the reduced mechanism of [12]. Excellent performance is observed for two model schemes with regard to both the extended mechanism and the reduced scheme of [12], and this is particularly encouraging for the shorter 14-species version. It should also be added that the overall performance of both models is compared very well with the calculations presented in [31] obtained with the extended GRI3.0 library.

The capability of the reduced models to capture the extinction states in a perfectly stirred reactor (PSR) was next tested for equivalence ratios ranging from $\phi = 0.25$ to 1.2 and inlet temperatures $T_0 = 300$–600 K, which are relevant to a range of applications [4, 5]. The blow-out residence time for a given value of $\phi$ was obtained by PSR simulations using CHEMKIN II [24]. Figure 7 shows the predictions of the lean blow-out (LBO) stability curve for a $CH_4$–air mixture at $p = 1$ atm and

$T_0$ = 300 K and provides a picture of the flame holding performance of each scheme. It can be observed that the four mechanisms display close LBO performance, although the stability curve predictions from the reduced kinetic models tend toward higher residence times, compared to the USC mechanism. The LBO bounds were found to be sensitive to the inclusion of a more complete $CO/H_2/O_2$ scheme, and this proved beneficial for the 14-species scheme behavior.

Subsequently the axisymmetric co-flowing lifted laminar jet flame [25, 26] was calculated for qualitative and quantitative reproduction of the temperature and major species fields, as well as the lift-off heights in this more complex burner arrangement. This is a severe test of the ability of the reduced schemes to capture the flame structure features more akin to practical combustors. The burner sketch is given in the inset in Fig. 8d.

The contours of temperature (Fig. 8a), and the $CO_2$ (Fig. 8b), CO (Fig. 8c), and $C_2H_2$ (Fig. 8d) species concentrations computed by the 22-species and 14-species models indicate that the produced distributions are in very close agreement with the counterpart plots provided in [25, 26]. The models have competently captured the lift-off position and flame heights for both the 40/60 and 65/35 methane dilutions, as seen from the calculated temperature contour plots (see Fig. 8a) [26], while the dispositions of all species including $CO_2$ and CO for the 65/35 flame [25] have also been reproduced quite successfully both in the near lifted base region and over the extent of the flame envelope. The computed spatial distributions of the minor species and $C_2H_2$ also agree very closely with the measured dispositions, while the lifted base exhibits the experimentally observed distinct wishbone structure, involving lean, rich, and stoichiometric branches.

The centerline temperature profiles for the 65/35 flame predicted by both models (not shown here for brevity) retrieve the experimental trend quite satisfactorily, both in the lifted-off flame and along the rich branch developing regions. The successful reproduction of the triple branch development in the flame base stems both from the adequate reproduction of the flame speed and from the inclusion of the C2 oxidation route in both model schemes.

From the above-performed comparisons, it appears that the presented reduced and simplified schemes produce an accurate and consistent behavior in predicting the target characteristics of (Section 1) over the investigated range of flame conditions. Some moderate discrepancies observed locally in the case of the quasi-global scheme for the richer mixtures are likely due to the insufficient number of intermediate hydrocarbons retained to represent the fuel decomposition.

## CONCLUSIONS

An effort was applied to develop two reduced chemical schemes for high-temperature oxidation of atmospheric methane flames over the range of equivalence ratios between 0.7 and 1.4 at preheat temperatures from 300 to 650 K. The presented short skeletal 22-species scheme with 103 reactions includes a significant section of both the C1 and C2 oxidation routes, important intermediates, major and minor radicals, as well as a detailed $CO/H_2/O_2$ subset. A compact quasi-global, 14-species scheme was further produced by modeling the methyl radical pool consumption toward $CH_2$ and CO through reactions with O and OH, and retaining a comprehensive $CO/H_2/O_2$ subset; the C2 chain with the recombination of $CH_3$ into $C_2H_6$ and the production of $C_2H_2$ was also represented in this shorter version.

The reaction rate coefficients of selected combined reactions in the produced schemes were expressed in a simple Arrhenius form, and the optimization process was targeted to adjustment of the pre-exponential constants. All global rates were parametrically fine-tuned by computing the flame properties of well-documented 0D and 1D premixed freely propagating and counterflow jet flames, as well as axisymmetric co-flowing laminar lifted partially premixed (triple) jet flames and comparing performance against full and reduced schemes from the literature.

The overall performance of the two schemes was found to be encouraging, with possible refinements, such as, e.g., addition of an $NO_x$ submodel; either scheme can be suitably employed in large-scale 3D turbulent combustion simulations, depending on the available computational resources.

Although the reduced kinetic schemes do not produce the amount of chemical information available with detailed kinetics, significant features of flame properties can be portrayed very adequately. The above-described procedure can be systematically extended to higher hydrocarbons or alternative fuels of technological interest.

The authors express their gratitude to Prof. Egolfopoulos and his team (Combustion and Fuels Research Laboratory, Department of Aerospace and Mechanical Engineering, University of Southern California, LA) for supplying the reduced 31-species scheme and for useful discussions on the paper.

## REFERENCES

1. T. Lu and C. K. Law, "Toward Accommodating Realistic Fuel Chemistry in Large-Scale Computations," Prog. Energy Combust. Sci. **35**, 192–215 (2009).

2. C. Z. Xiouris and P. Koutmos, "Fluid Dynamics Modeling of a Stratified Disk Burner in Swirl Co-Flow," Appl. Therm. Eng. **35**, 60–70 (2012).
3. F. Proch and A. M. Kempf, "Numerical Analysis of the Cambridge Stratified Flame Series Using Artificial Thickened Flame LES with Tabulated Premixed Flame Chemistry," Combust. Flame **161**, 2627–2646 (2014).
4. P. Gokulakrishnan, S. Kwon, A. J. Hamer, et al., "Reduced Kinetic Mechanism for Reactive Flow Simulation of Syngas/Methane Combustion at Gas Turbine Conditions," in *ASME Turbo Expo 2006: Power for Land, Sea, and Air* (2006), pp. 513–521.
5. B. Franzelli, E. Riber, L. Y. M. Gicquel, and T. Poinsot, "Large Eddy Simulation of Combustion Instabilities in a Lean Partially Premixed Swirled Flame," Combust. Flame **159**, 621–637 (2012).
6. G. Bulat, E. Fedina, C. Fureby, W. Meier, and U. Stopper, "Reacting Flow in an Industrial Gas Turbine Combustor: Les and Experimental Analysis," Proc. Combust. Inst. **35**, 175–3183 (2015).
7. J. Bibrzycki, T. Poinsot, and A. Zajdel, "Investigation of Laminar Flame Speed of $CH_4/N_2/O_2$ and $CH_4/CO_2/O_2$ Mixtures Using Reduced Chemical Kinetic Mechanisms," Arch. Combust., 287–296 (2010).
8. H. Wang, X. You, A. V. Joshi, et al., "USC Mech Version II. High-Temperature Combustion Reaction Model of $H_2$/CO/C1–C4 Compounds," 2007.
9. C. K. Law, C. J. Sung, H. Wang, and T. F. Lu, "Development of Comprehensive Detailed and Reduced Reaction Mechanisms for Combustion Modeling," AIAA J. **41**, 1629–1646 (2003).
10. F. Mauss and N. Peters, "Reduced Kinetic Mechanisms for Premixed Methane–Air Flames," in *Reduced Kinetic Mechanisms for Application in Combustion Systems*, Ed. by N. Peters and B. Rogg (Springer, Heidelberg–Berlin, 1993).
11. A. L. Sanchez, A. Lepinette, M. Bollig, et al., "The Reduced Kinetic Description of Lean Premixed Combustion," Combust. Flame **123**, 436–464 (2000).
12. T. Lu and C. K. Law, "A Criterion Based on Computational Singular Perturbation for the Identification of Quasi Steady State Species: A Reduced Mechanism for Methane Oxidation with NO Chemistry," Combust. Flame **154**, 761–774 (2008).
13. U. Maas and S. B. Pope, "Simplifying Chemical Kinetics: Intrinsic Low-Dimensional Manifolds in Composition Space," Combust. Flame **88**, 239–264 (1992).
14. M. F. Karalus, K. B. Fackler, I. V. Novosselov, et al., "A Skeletal Mechanism for the Reactive Flow Simulation of Methane Combustion," Combust. Fuels Emiss. (2013).
15. A. Kazakov and M. Frenklach, "Reduced Reaction Sets Based on GRI-Mech 1.2," (n.d.); http://www.me.berkeley.edu/drm/.
16. M. D. Smooke, V. Giovangigli, *Reduced Kinetic Mechanisms and Asymptotic Approximations for Methane–Air Flames*, (Springer, Berlin, Heidelberg, 1991).
17. H. P. Mallampalli, T. H. Fletcher, and J. Y. Chen, "Evaluation of $CH_4/NO_x$ Reduced Mechanisms Used for Modeling Lean Premixed Turbulent Combustion of Natural Gas," J. Eng. Gas Turbines Power. **120**, 703–712 (1998); http://dx.doi.org/10.1115/1.2818457. .
18. P. Koutmos and S. Dimopoulos, "A Reduced Multi-Step Integrated Oxidation Scheme for Methane Suitable for Use into Complex Reactive Flow Calculations," Comput. Assist. Mech. Eng. Sci. **12**, 17–30 (2005).
19. C. K. Westbrook and F. L. Dryer, "Chemical Kinetic Modeling of Hydrocarbon Combustion," Prog. Energy Combust. Sci. **10**, 1–57 (1984).
20. F. Egolfopoulos and R. Zhao, Private Communication 90089-1453 (Dep. Aerosp. Mech. Eng., Univ. South. California, Los Angeles, 2015).
21. K. Souflas et al., "Determination of Laminar Flame Speeds using Axisymmetric Bunsen Flames: Intricacies and Accuracy," in *9th Mediter. Combust. Symp.* (2015).
22. A. Arvidsson, *Development of an Automatic Reduction Tool for Chemical Mechanisms and an Optimized Sparse Matrix Solver for Systems of Differential and Algebraic Equations* (Lund University, 2010).
23. J. Huang and W. K. Bushe, "Experimental and Kinetic Study of Autoignition in Methane/Ethane/Air and Methane/Propane/Air Mixtures under Engine-Relevant Conditions," Combust. Flame **144**, 74–88 (2006).
24. *Chemkin II Collection, Release 4.1* (2006).
25. C. S. McEnally, L. D. Pfefferle, A. M. Schaffer, et al., "Characterization of a Coflowing Methane/Air Non-Premixed Flame with Computer Modeling, Rayleigh–Raman Imaging, and On-Line Mass Spectrometry," Proc. Combust. Inst. **28**, 2063–2070 (2000).
26. K. T. Walsh, J. Fielding, M. D. Smooke, and M. B. Long, "Experimental and Computational Study of Temperature, Species, and Soot in Buoyant and Non-Buoyant Coflow Laminar Diffusion Flames," Proc. Combust. Inst. **28**, 1973–1979 (2000).
27. *ANSYS®Academic Research, Release 18* (2017).
28. E. Hu, X. Li, X. Meng, et al., "Laminar Flame Speeds and Ignition Delay Times of Methane–Air Mixtures at Elevated Temperatures and Pressures," Fuel **158**, 1–10 (2015).
29. O. Park, P. S. Veloo, N. Liu, and F. N. Egolfopoulos, "Combustion Characteristics of Alternative Gaseous Fuels," Proc. Combust. Inst. **33**, 887–894 (2011).
30. Y. Wu, V. Modica, B. Rossow, and F. Grisch, "Effects of Pressure and Preheating Temperature on the Laminar Flame Speed of Methane/Air and Acetone/Air Mixtures," Fuel **185**, 577–588 (2016).
31. Z. Cheng, J. A. Wehrmeyer, and R. W. Pitz, "Lean or Ultra-Lean Stretched Planar Methane/Air Flames," Proc. Combust. Inst. **30**, 285–292 (2005).

# APPENDIX

## 22-species model

ELEMENTS

O H C N

SPECIES

H O OH $HO_2$ $H_2$ $H_2O$ $O_2$ CO $CO_2$ HCO

$CH_2O$ $CH_2$ $CH_3$ $CH_4$ $CH_2OH$ $C_2O$ $C_2H_2$ $C_2H_3$ $C_2H_4$ $C_2H_5$ $C_2H_6$ $N_2$

| No. | Reaction | $A$, $cm^3$, mol, s | $n$ | $E$, J/mol |
|---|---|---|---|---|
| 1 | $H + O_2 \leftrightarrow O + OH$ | $2.644 \cdot 10^{16}$ | −0.671 | 17 041.00 |
| 2 | $O + H_2 \leftrightarrow H + OH$ | $4.589 \cdot 10^{4}$ | 2.700 | 6260.00 |
| 3 | $OH + H_2 \leftrightarrow H + H_2O$ | $1.734 \cdot 10^{8}$ | 1.510 | 3430.00 |
| 4 | $2OH \leftrightarrow O + H_2O$ | $3.973 \cdot 10^{4}$ | 2.400 | −2110.00 |
| 5 | $2H + M \leftrightarrow H_2 + M$ | $1.780 \cdot 10^{18}$ | −1.000 | 0 |
| $H_2/0/H_2O/0/CO_2/0/$ | | | | |
| 6 | $2H + H_2 \leftrightarrow 2H_2$ | $9.000 \cdot 10^{16}$ | −0.600 | 0 |
| 7 | $2H + H_2O \leftrightarrow H_2 + H_2O$ | $5.624 \cdot 10^{19}$ | −1.250 | 0 |
| 8 | $2H + CO_2 \leftrightarrow H_2 + CO_2$ | $5.500 \cdot 10^{20}$ | −2.000 | 0 |
| 9 | $H + OH + M \leftrightarrow H_2O + M$ | $4.400 \cdot 10^{22}$ | −2.000 | 0 |
| $H_2/2.00/H_2O/6.30/CO/1.75/CO_2/3.60/$ | | | | |
| 10 | $O + H + M \leftrightarrow OH + M$ | $9.428 \cdot 10^{18}$ | −1.000 | 0 |
| $H_2/2.00/H_2O/12.00/CO/1.75/CO_2/3.60/$ | | | | |
| 11 | $2O + M \leftrightarrow O_2 + M$ | $1.200 \cdot 10^{17}$ | −1.000 | 0 |
| $H_2/2.40/H_2O/15.40/CO/1.75/CO_2/3.60/$ | | | | |
| 12 | $H + O_2(+M) \leftrightarrow HO_2(+M)$ | $5.116 \cdot 10^{12}$ | 0.440 | 0 |
| LOW / $0.63280 \cdot 10^{20}$ $-0.14000 \cdot 10^{1}$ $0 \cdot 10^{0}$ / | | | | |
| TROE / $0.50000 \cdot 10^{0}$ $0.10000 \cdot 10^{-29}$ $0.10000 \cdot 10^{31}$ / | | | | |
| $H_2O/11.89/O_2/0.85/CO/1.09/CO_2/2.18/$ | | | | |
| 13 | $H_2 + O_2 \leftrightarrow HO_2 + H$ | $5.916 \cdot 10^{5}$ | 2.433 | 53 502.00 |
| 14 | $HO_2 + H \leftrightarrow O + H_2O$ | $3.970 \cdot 10^{12}$ | 0 | 671.00 |
| 15 | $HO_2 + H \leftrightarrow 2OH$ | $7.485 \cdot 10^{13}$ | 0 | 295.00 |
| 16 | $HO_2 + O \leftrightarrow OH + O_2$ | $4.000 \cdot 10^{13}$ | 0 | 0 |
| 17 | $OH + HO_2 \leftrightarrow H_2O + O_2$ | $1.410 \cdot 10^{18}$ | −1.760 | 60.00 |

| No. | Reaction | $A$, $cm^3$, mol, s | $n$ | $E$, J/mol |
|---|---|---|---|---|
| DUPLICATE | | | | |
| 18 | $OH + HO_2 \leftrightarrow H_2O + O_2$ | $1.120 \cdot 10^{85}$ | −22.300 | 26 900.00 |
| DUPLICATE | | | | |
| 19 | $OH + HO_2 \leftrightarrow H_2O + O_2$ | $5.370 \cdot 10^{70}$ | −16.720 | 32 900.00 |
| DUPLICATE | | | | |
| 20 | $OH + HO_2 \leftrightarrow H_2O + O_2$ | $2.510 \cdot 10^{12}$ | 2.000 | 40 000.00 |
| DUPLICATE | | | | |
| 21 | $OH + HO_2 \leftrightarrow H_2O + O_2$ | $1.000 \cdot 10^{136}$ | −40.000 | 34 800.00 |
| DUPLICATE | | | | |
| 22 | $CO + O(+M) \leftrightarrow CO_2(+M)$ | $1.362 \cdot 10^{10}$ | 0 | 2384.00 |
| LOW / $0.11730 \cdot 10^{25}$ $-0.27900 \cdot 10^{1}$ $0.41910 \cdot 10^{4}$ / | | | | |
| $H_2$/2.00/$H_2O$/12.00/CO/1.75/$CO_2$/3.60/ | | | | |
| 23 | $CO + OH \leftrightarrow CO_2 + H$ | $7.046 \cdot 10^{4}$ | 2.053 | −355.67 |
| 24 | $CO + O_2 \leftrightarrow CO_2 + O$ | $1.119 \cdot 10^{12}$ | 0 | 47 700.00 |
| 25 | $CO + HO_2 \leftrightarrow CO_2 + OH$ | $1.570 \cdot 10^{5}$ | 2.180 | 17 942.61 |
| 26 | $HCO + H \leftrightarrow CO + H_2$ | $1.200 \cdot 10^{14}$ | 0 | 0 |
| 27 | $HCO + O \leftrightarrow CO + OH$ | $3.000 \cdot 10^{13}$ | 0 | 0 |
| 28 | $HCO + O \leftrightarrow CO_2 + H$ | $3.000 \cdot 10^{13}$ | 0 | 0 |
| 29 | $HCO + OH \leftrightarrow CO + H_2O$ | $3.020 \cdot 10^{13}$ | 0 | 0 |
| 30 | $HCO + M \leftrightarrow CO + H + M$ | $1.870 \cdot 10^{17}$ | −1.000 | 17 000.00 |
| $H_2$/2.00/$H_2O$/0/CO/1.75/$CO_2$/3.60/ | | | | |
| 31 | $HCO + H_2O \leftrightarrow CO + H + H_2O$ | $2.244 \cdot 10^{18}$ | −1.000 | 17 000.00 |
| 32 | $HCO + O_2 \leftrightarrow CO + HO_2$ | $1.204 \cdot 10^{10}$ | 0.807 | −727.00 |
| 33 | $CO + H_2(+M) \leftrightarrow CH_2O(+M)$ | $4.300 \cdot 10^{7}$ | 1.500 | 79 600.00 |
| LOW / $0.50700 \cdot 10^{28}$ $-0.34200 \cdot 10^{1}$ $0.84350 \cdot 10^{5}$ / | | | | |
| TROE / $0.93200 \cdot 10^{0}$ $0.19700 \cdot 10^{3}$ $0.15400 \cdot 10^{4}$ $0.10300 \cdot 10^{5}$ / | | | | |
| $H_2$/2.00/$H_2O$/6.00/CO/1.50/$CO_2$/2.00/$CH_4$/2.00/$C_2H_6$/3.00/ | | | | |
| 34 | $HCO + H(+M) \leftrightarrow CH_2O(+M)$ | $1.090 \cdot 10^{12}$ | 0.480 | −260.00 |
| LOW / $0.13500 \cdot 10^{25}$ $-0.25700 \cdot 10^{1}$ $0.14250 \cdot 10^{4}$ / | | | | |
| TROE / $0.7824 \cdot 10^{0}$ $0.27100 \cdot 10^{3}$ $0.27550 \cdot 10^{4}$ $0.65700 \cdot 10^{4}$ / | | | | |
| $H_2$/2.00/$H_2O$/6.00/CO/1.50/$CO_2$/2.00/$CH_4$/2.00/$C_2H_6$/3.00/ | | | | |
| 35 | $CH_2 + H(+M) \leftrightarrow CH_3(+M)$ | $2.500 \cdot 10^{16}$ | −0.800 | 0 |

| No. | Reaction | $A$, $cm^3$, mol, s | $n$ | $E$, J/mol |
|---|---|---|---|---|
| LOW / $0.32000 \cdot 10^{28}$ $-0.31400 \cdot 10^{1}$ $0.12300 \cdot 10^{4}$ / | | | | |
| TROE / $0.68000 \cdot 10^{0}$ $0.78000 \cdot 10^{2}$ $0.19950 \cdot 10^{4}$ $0.55900 \cdot 10^{4}$ / | | | | |
| $H_2$/2.00/$H_2O$/6.00/CO/1.50/$CO_2$/2.00/$CH_4$/2.00/$C_2H_6$/3.00/ | | | | |
| 36 | $CH_2 + O \leftrightarrow HCO + H$ | $8.000 \cdot 10^{13}$ | 0 | 0 |
| 37 | $CH_2 + OH \leftrightarrow CH_2O + H$ | $2.000 \cdot 10^{13}$ | 0 | 0 |
| 38 | $CH_2 + H_2 \leftrightarrow H + CH_3$ | $5.000 \cdot 10^{5}$ | 2.000 | 7230.00 |
| 39 | $CH_2 + O_2 \leftrightarrow HCO + OH$ | $1.060 \cdot 10^{13}$ | 0 | 1500.00 |
| 40 | $CH_2 + O_2 \leftrightarrow CO_2 + 2H$ | $2.640 \cdot 10^{12}$ | 0 | 1500.00 |
| 41 | $CH_2 + HO_2 \leftrightarrow CH_2O + OH$ | $2.000 \cdot 10^{13}$ | 0 | 0 |
| 42 | $2CH_2 \leftrightarrow C_2H_2 + H_2$ | $3.200 \cdot 10^{13}$ | 0 | 0 |
| 43 | $CH_2O + H(+M) \leftrightarrow CH_2OH(+M)$ | $5.400 \cdot 10^{11}$ | 0.454 | 3600.00 |
| LOW / $0.12700 \cdot 10^{33}$ $-0.48200 \cdot 10^{1}$ $0.65300 \cdot 10^{4}$ / | | | | |
| TROE / $0.71870 \cdot 10^{0}$ $0.10300 \cdot 10^{3}$ $0.12910 \cdot 10^{4}$ $0.41600 \cdot 10^{4}$ / | | | | |
| $H_2$/2.00/$H_2O$/6.00/CO/1.50/$CO_2$/2.00/$CH_4$/2.00/$C_2H_6$/3.00/ | | | | |
| 44 | $CH_2O + H \leftrightarrow HCO + H_2$ | $2.300 \cdot 10^{10}$ | 1.050 | 3275.00 |
| 45 | $CH_2O + O \leftrightarrow HCO + OH$ | $3.900 \cdot 10^{13}$ | 0 | 3540.00 |
| 46 | $CH_2O + OH \leftrightarrow HCO + H_2O$ | $3.430 \cdot 10^{9}$ | 1.180 | −447.00 |
| 47 | $CH_2O + O_2 \leftrightarrow HCO + HO_2$ | $1.000 \cdot 10^{14}$ | 0 | 40 000.00 |
| 48 | $CH_3 + H(+M) \leftrightarrow CH_4(+M)$ | $1.270 \cdot 10^{16}$ | −0.630 | 383.00 |
| LOW / $0.24770 \cdot 10^{34}$ $-0.47600 \cdot 10^{1}$ $0.24400 \cdot 10^{4}$ / | | | | |
| TROE / $0.78300 \cdot 10^{0}$ $0.74000 \cdot 10^{2}$ $0.29410 \cdot 10^{4}$ $0.69640 \cdot 10^{4}$ / | | | | |
| $H_2$/2.00/$H_2O$/6.00/CO/1.50/$CO_2$/2.00/$CH_4$/2.00/$C_2H_6$/3.00/ | | | | |
| 49 | $CH_3 + O \leftrightarrow CH_2O + H$ | $8.430 \cdot 10^{13}$ | 0 | 0 |
| 50 | $CH_3 + OH \leftrightarrow CH_2 + H_2O$ | $9.300 \cdot 10^{8}$ | 1.600 | 5420.00 |
| 51 | $CH_3 + O_2 \leftrightarrow OH + CH_2O$ | $3.600 \cdot 10^{10}$ | 0 | 8940.00 |
| 52 | $CH_3 + HCO \leftrightarrow CH_4 + CO$ | $8.480 \cdot 10^{12}$ | 0 | 0 |
| 53 | $CH_3 + CH_2O \leftrightarrow CH_4 + HCO$ | $3.320 \cdot 10^{3}$ | 2.810 | 5860.00 |
| 54 | $CH_3 + CH_2 \leftrightarrow C_2H_4 + H$ | $4.000 \cdot 10^{13}$ | 0 | 0 |
| 55 | $CH_3 + HO_2 \leftrightarrow CH_4 + O_2$ | $1.000 \cdot 10^{12}$ | 0 | 0 |
| 56 | $2CH_3(+M) \leftrightarrow C_2H_6(+M)$ | $2.120 \cdot 10^{16}$ | −0.970 | 620.00 |
| LOW / $0.17700 \cdot 10^{51}$ $-0.96700 \cdot 10^{1}$ $0.62200 \cdot 10^{4}$ / | | | | |
| TROE / $0.53250 \cdot 10^{0}$ $0.15100 \cdot 10^{3}$ $0.10380 \cdot 10^{4}$ $0.49700 \cdot 10^{4}$ / | | | | |
| $H_2$/2.00/$H_2O$/6.00/CO/1.50/$CO_2$/2.00/$CH_4$/2.00/$C_2H_6$/3.00/ | | | | |
| 57 | $2CH_3 \leftrightarrow H + C_2H_5$ | $4.990 \cdot 10^{12}$ | 0.100 | 10 600.00 |
| 58 | $CH_2OH + H \leftrightarrow CH_2O + H_2$ | $2.000 \cdot 10^{13}$ | 0 | 0 |
| 59 | $CH_2OH + H \leftrightarrow CH_3 + OH$ | $1.200 \cdot 10^{13}$ | 0 | 0 |
| 60 | $CH_2OH + O \leftrightarrow CH_2O + OH$ | $1.000 \cdot 10^{13}$ | 0 | 0 |

| No. | Reaction | $A$, $cm^3$, mol, s | $n$ | $E$, J/mol |
|---|---|---|---|---|
| 61 | $CH_2OH + OH \leftrightarrow CH_2O + H_2O$ | $5.000 \cdot 10^{12}$ | 0 | 0 |
| 62 | $CH_2OH + O_2 \leftrightarrow CH_2O + HO_2$ | $1.800 \cdot 10^{13}$ | 0 | 900.00 |
| 63 | $CH_4 + H \leftrightarrow CH_3 + H_2$ | $6.600 \cdot 10^{8}$ | 1.620 | 10 840.00 |
| 64 | $CH_4 + O \leftrightarrow CH_3 + OH$ | $1.020 \cdot 10^{9}$ | 1.500 | 8600.00 |
| 65 | $CH_4 + OH \leftrightarrow CH_3 + H_2O$ | $1.000 \cdot 10^{8}$ | 1.600 | 3120.00 |
| 66 | $CH_4 + CH_2 \leftrightarrow 2CH_3$ | $2.460 \cdot 10^{6}$ | 2.000 | 8270.00 |
| 67 | $CH_4 + 2O_2 \leftrightarrow CO + 2OH + H_2O$ | $9.500 \cdot 10^{13}$ | 1.550 | 40 000.00 |
| 68 | $C_2O + O \leftrightarrow 2CO$ | $5.000 \cdot 10^{13}$ | 0 | 0 |
| 69 | $C_2O + OH \leftrightarrow 2CO + H$ | $2.000 \cdot 10^{13}$ | 0 | 0 |
| 70 | $C_2O + O_2 \leftrightarrow 2CO + O$ | $2.000 \cdot 10^{13}$ | 0 | 0 |
| 71 | $C_2H_3(+M) \leftrightarrow C_2H_2 + H(+M)$ | $3.860 \cdot 10^{8}$ | 1.620 | 37 048.20 |
| LOW / $0.25650 \cdot 10^{28}$ $-0.34000 \cdot 10^{1}$ $0.35799 \cdot 10^{5}$ / | | | | |
| TROE / $0.19816 \cdot 10^{1}$ $0.53837 \cdot 10^{4}$ $0.42932 \cdot 10^{1}$ $-0.79500 \cdot 10^{-1}$ / | | | | |
| $H_2$/2.00/$H_2O$/6.00/CO/1.50/$CO_2$/2.00/$CH_4$/2.00/$C_2H_2$/3.00/ | | | | |
| $C_2H_4$/3.00/$C_2H_6$/3.00/ | | | | |
| 72 | $C_2H_2 + O \leftrightarrow CH_2 + CO$ | $4.080 \cdot 10^{6}$ | 2.000 | 1900.00 |
| 73 | $C_2H_2 + OH \leftrightarrow CH_3 + CO$ | $4.830 \cdot 10^{-4}$ | 4.000 | −2000.00 |
| 74 | $C_2H_2 + HCO \leftrightarrow C_2H_3 + CO$ | $1.000 \cdot 10^{7}$ | 2.000 | 6000.00 |
| 75 | $C_2H_3 + H(+M) \leftrightarrow C_2H_4(+M)$ | $6.080 \cdot 10^{12}$ | 0.270 | 280.00 |
| LOW / $0.14000 \cdot 10^{31}$ $-0.38600 \cdot 10^{1}$ $0.33200 \cdot 10^{4}$ / | | | | |
| TROE / $0.78200 \cdot 10^{0}$ $0.20750 \cdot 10^{3}$ $0.26630 \cdot 10^{4}$ $0.60950 \cdot 10^{4}$ / | | | | |
| $H_2$/2.00/$H_2O$/6.00/CO/1.50/$CO_2$/2.00/$CH_4$/2.00/$C_2H_2$/3.00/ | | | | |
| $C_2H_4$/3.00/$C_2H_6$/3.00/ | | | | |
| 76 | $C_2H_3 + H \leftrightarrow C_2H_2 + H_2$ | $9.000 \cdot 10^{13}$ | 0 | 0 |
| 77 | $C_2H_3 + O \leftrightarrow CH_3 + CO$ | $4.800 \cdot 10^{13}$ | 0 | 0 |
| 78 | $C_2H_3 + OH \leftrightarrow C_2H_2 + H_2O$ | $3.011 \cdot 10^{13}$ | 0 | 0 |
| 79 | $C_2H_3 + O_2 \leftrightarrow C_2H_2 + HO_2$ | $1.340 \cdot 10^{6}$ | 1.610 | −383.40 |
| 80 | $C_2H_3 + O_2 \leftrightarrow HCO + CH_2O$ | $4.600 \cdot 10^{16}$ | −1.390 | 1010.00 |
| 81 | $C_2H_3 + HCO \leftrightarrow C_2H_4 + CO$ | $9.033 \cdot 10^{13}$ | 0 | 0 |
| 82 | $C_2H_3 + CH_3 \leftrightarrow C_2H_2 + CH_4$ | $3.920 \cdot 10^{11}$ | 0 | 0 |
| 83 | $2C_2H_3 \leftrightarrow C_2H_2 + C_2H_4$ | $9.600 \cdot 10^{11}$ | 0 | 0 |
| 84 | $C_2H_4 + H(+M) \leftrightarrow C_2H_5(+M)$ | $1.367 \cdot 10^{9}$ | 1.463 | 1355.00 |
| LOW / $0.20270 \cdot 10^{40}$ $-0.66420 \cdot 10^{1}$ $0.57690 \cdot 10^{4}$ / | | | | |
| TROE / $0.15690 \cdot 10^{1}$ $-0.91470 \cdot 10^{4}$ $0.29900 \cdot 10^{3}$ $0.15240 \cdot 10^{3}$ / | | | | |
| $H_2$/2.00/$H_2O$/6.00/CO/1.50/$CO_2$/2.00/$CH_4$/2.00/$C_2H_6$/3.00/ | | | | |

| No. | Reaction | $A$, $cm^3$, mol, s | $n$ | $E$, J/mol |
|---|---|---|---|---|
| 85 | $C_2H_4 + H \leftrightarrow C_2H_3 + H_2$ | $5.070 \cdot 10^7$ | 1.900 | 12 950.00 |
| 86 | $C_2H_4 + O \leftrightarrow C_2H_3 + OH$ | $1.510 \cdot 10^7$ | 1.900 | 3740.00 |
| 87 | $C_2H_4 + O \leftrightarrow CH_3 + HCO$ | $1.920 \cdot 10^7$ | 1.830 | 220.00 |
| 88 | $C_2H_4 + O \leftrightarrow CH_2 + CH_2O$ | $3.840 \cdot 10^5$ | 1.830 | 220.00 |
| 89 | $C_2H_4 + OH \leftrightarrow C_2H_3 + H_2O$ | $3.600 \cdot 10^6$ | 2.000 | 2500.00 |
| 90 | $C_2H_4 + HCO \leftrightarrow C_2H_5 + CO$ | $1.000 \cdot 10^7$ | 2.000 | 8000.00 |
| 91 | $C_2H_4 + CH_3 \leftrightarrow C_2H_3 + CH_4$ | $2.270 \cdot 10^5$ | 2.000 | 9200.00 |
| 92 | $C_2H_4 + O_2 \leftrightarrow C_2H_3 + HO_2$ | $4.220 \cdot 10^{13}$ | 0 | 60 800.00 |
| 93 | $C_2H_5 + H(+M) \leftrightarrow C_2H_6(+M)$ | $5.210 \cdot 10^{17}$ | −0.990 | 1580.00 |
| LOW / $0.19900 \cdot 10^{42}$ $-0.70800 \cdot 10^1$ $0.66850 \cdot 10^4$ / | | | | |
| TROE / $0.84220 \cdot 10^0$ $0.12500 \cdot 10^3$ $0.22190 \cdot 10^4$ $0.68820 \cdot 10^4$ / | | | | |
| $H_2$/2.00/$H_2O$/6.00/CO/1.50/$CO_2$/2.00/$CH_4$/2.00/$C_2H_6$/3.00/ | | | | |
| 94 | $C_2H_5 + H \leftrightarrow C_2H_4 + H_2$ | $2.000 \cdot 10^{12}$ | 0 | 0 |
| 95 | $C_2H_5 + O \leftrightarrow CH_3 + CH_2O$ | $1.604 \cdot 10^{13}$ | 0 | 0 |
| 96 | $C_2H_5 + O_2 \leftrightarrow C_2H_4 + HO_2$ | $2.000 \cdot 10^{10}$ | 0 | 0 |
| 97 | $C_2H_5 + HO_2 \leftrightarrow C_2H_6 + O_2$ | $3.000 \cdot 10^{11}$ | 0 | 0 |
| 98 | $C_2H_5 + HO_2 \leftrightarrow CH_3 + CH_2O + OH$ | $2.400 \cdot 10^{13}$ | 0 | 0 |
| 99 | $C_2H_6 + H \leftrightarrow C_2H_5 + H_2$ | $1.150 \cdot 10^8$ | 1.900 | 7530.00 |
| 100 | $C_2H_6 + O \leftrightarrow C_2H_5 + OH$ | $8.980 \cdot 10^7$ | 1.920 | 5690.00 |
| 101 | $C_2H_6 + OH \leftrightarrow C_2H_5 + H_2O$ | $3.540 \cdot 10^6$ | 2.120 | 870.00 |
| 102 | $C_2H_6 + CH_3 \leftrightarrow C_2H_5 + CH_4$ | $6.140 \cdot 10^6$ | 1.740 | 10 450.00 |

### 14-species model

ELEMENTS

O H C N

SPECIES

$H_2$ H O $O_2$ OH $H_2O$ $CH_2$ $CH_3$ $CH_4$ CO $CO_2$ $C_2H_6$ $C_2H_2$ $N_2$

| No. | Reaction | $A$, $cm^3$, mol, s | $n$ | $E$, J/mol |
|---|---|---|---|---|
| 1 | $2H + H_2O \leftrightarrow H_2 + H_2O$ | $5.624 \cdot 10^{20}$ | −1.250 | 0 |
| 2 | $H + O_2 \leftrightarrow O + OH$ | $2.644 \cdot 10^{16}$ | −0.671 | 17 041.00 |
| 3 | $O + H_2 \leftrightarrow H + OH$ | $4.589 \cdot 10^4$ | 2.700 | 6260.00 |
| 4 | $OH + H_2 \leftrightarrow H + H_2O$ | $1.734 \cdot 10^8$ | 1.510 | 3430.00 |
| 5 | $2OH \leftrightarrow O + H_2O$ | $3.973 \cdot 10^4$ | 2.400 | −2110.00 |
| 6 | $2H + M \leftrightarrow H_2 + M$ | $1.780 \cdot 10^{20}$ | −1.000 | 0 |
| $H_2$/0/$H_2O$/0/$CO_2$/0/ | | | | |

| No. | Reaction | $A$, $cm^3$, mol, s | $n$ | $E$, J/mol |
|---|---|---|---|---|
| 7 | $H + OH + M \leftrightarrow H_2O + M$ | $4.400 \cdot 10^{22}$ | $-2.000$ | 0 |
| $H_2/2.00/H_2O/6.30/CO/1.75/CO_2/3.60/$ | | | | |
| 8 | $O + H + M \leftrightarrow OH + M$ | $9.428 \cdot 10^{18}$ | $-1.000$ | 0 |
| $H_2/2.00/H_2O/12.00/CO/1.75/CO_2/3.60/$ | | | | |
| 9 | $2O + M \leftrightarrow O_2 + M$ | $1.200 \cdot 10^{17}$ | $-1.000$ | 0 |
| $H_2/2.40/H_2O/15.40/CO/1.75/CO_2/3.60/$ | | | | |
| 10 | $CO + O(+M) \leftrightarrow CO_2(+M)$ | $1.362 \cdot 10^{10}$ | 0 | 2384.00 |
| LOW / $0.11730 \cdot 10^{25}$ $-0.27900 \cdot 10^{1}$ $0.41910 \cdot 10^{4}$ / | | | | |
| $H_2/2.00/H_2O/12.00/CO/1.75/CO_2/3.60/$ | | | | |
| 11 | $CO + OH \leftrightarrow CO_2 + H$ | $7.046 \cdot 10^{4}$ | 2.053 | $-355.67$ |
| 12 | $CO + O_2 \leftrightarrow CO_2 + O$ | $1.119 \cdot 10^{12}$ | 0 | 47 700.00 |
| 13 | $CH_2 + H(+M) \leftrightarrow CH_3(+M)$ | $2.500 \cdot 10^{16}$ | $-0.800$ | 0 |
| LOW / $0.32000 \cdot 10^{28}$ $-0.31400 \cdot 10^{1}$ $0.12300 \cdot 10^{4}$ / | | | | |
| TROE / $0.68000 \cdot 10^{0}$ $0.78000 \cdot 10^{2}$ $0.19950 \cdot 10^{4}$ $0.55900 \cdot 10^{4}$ / | | | | |
| $H_2/2.00/H_2O/6.00/CO/1.50/CO_2/2.00/CH_4/2.00/C_2H_6/3.00/$ | | | | |
| 14 | $CH_2 + H_2 \leftrightarrow H + CH_3$ | $5.000 \cdot 10^{5}$ | 2.000 | 7230.00 |
| 15 | $CH_2 + CH_4 \leftrightarrow 2CH_3$ | $2.460 \cdot 10^{7}$ | 2.000 | 8270.00 |
| 16 | $CH_2 + O \leftrightarrow CO + 2H$ | $8.000 \cdot 10^{13}$ | 0 | 0 |
| 17 | $CH_2 + O_2 \leftrightarrow CO + OH + H$ | $1.060 \cdot 10^{13}$ | 0 | 1500.00 |
| 18 | $2CH_2 \leftrightarrow H_2 + C_2H_2$ | $1.300 \cdot 10^{15}$ | 0 | 11 944.00 |
| 19 | $CH_3 + OH \leftrightarrow CH_2 + H_2O$ | $1.350 \cdot 10^{9}$ | 1.600 | 5420.00 |
| 20 | $CH_3 + 2O \leftrightarrow CO + OH + H_2$ | $3.100 \cdot 10^{21}$ | 0 | 0 |
| 21 | $CH_3 + H(+M) \leftrightarrow CH_4(+M)$ | $1.270 \cdot 10^{16}$ | $-0.630$ | 383.00 |
| LOW / $0.24770 \cdot 10^{34}$ $-0.47600 \cdot 10^{1}$ $0.24400 \cdot 10^{4}$ / | | | | |
| TROE / $0.78300 \cdot 10^{0}$ $0.74000 \cdot 10^{2}$ $0.29410 \cdot 10^{4}$ $0.69640 \cdot 10^{4}$ / | | | | |
| $H_2/2.00/H_2O/6.00/CO/1.50/CO_2/2.00/CH_4/2.00/C_2H_6/3.00/$ | | | | |
| 22 | $C_2H_2 + O \leftrightarrow CO + CH_2$ | $9.940 \cdot 10^{5}$ | 2.000 | 1900.00 |
| 23 | $C_2H_6 + 4H \leftrightarrow C_2H_2 + 4H_2$ | $3.000 \cdot 10^{13}$ | 0 | 0 |
| 24 | $2CH_3(+M) \leftrightarrow C_2H_6(+M)$ | $6.770 \cdot 10^{16}$ | $-1.180$ | 654.00 |
| LOW / $3.400 \cdot 10^{41}$ $-7.030$ 2762.00/ | | | | |
| TROE/ 0.6190 73.20 1180.00 9999.00 / | | | | |
| $H_2/2.00/H_2O/6.00/CH_4/2.00/CO/1.50/CO_2/2.00/C_2H_6/3.00/$ | | | | |
| 25 | $CH_4 + O \leftrightarrow CH_3 + OH$ | $1.020 \cdot 10^{9}$ | 1.500 | 8600.00 |
| 26 | $CH_4 + H \leftrightarrow CH_3 + H_2$ | $6.600 \cdot 10^{8}$ | 1.620 | 10 840.00 |
| 27 | $CH_4 + OH \leftrightarrow CH_3 + H_2O$ | $1.000 \cdot 10^{8}$ | 1.600 | 3120.00 |
| 28 | $CH_4 + 2O_2 \leftrightarrow CO + 2OH + H_2O$ | $1.500 \cdot 10^{14}$ | 1.550 | 40 000.00 |